Analytical Methods

Accepted Manuscript

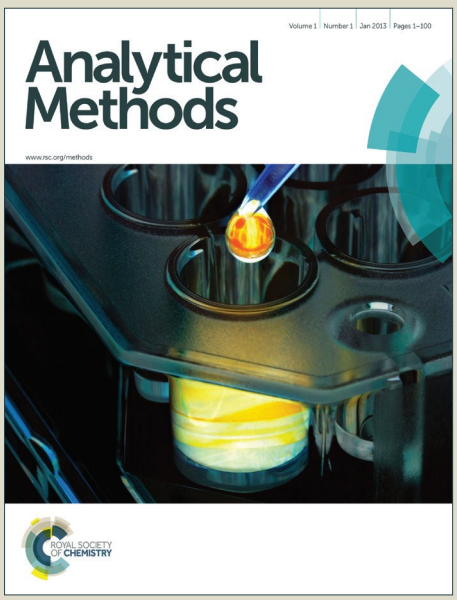

This is an *Accepted Manuscript*, which has been through the Royal Society of Chemistry peer review process and has been accepted for publication.

Accepted Manuscripts are published online shortly after acceptance, before technical editing, formatting and proof reading. Using this free service, authors can make their results available to the community, in citable form, before we publish the edited article. We will replace this *Accepted Manuscript* with the edited and formatted *Advance Article* as soon as it is available.

You can find more information about *Accepted Manuscripts* in the Information for Authors.

Please note that technical editing may introduce minor changes to the text and/or graphics, which may alter content. The journal's standard Terms & Conditions and the Ethical guidelines still apply. In no event shall the Royal Society of Chemistry be held responsible for any errors or omissions in this *Accepted Manuscript* or any consequences arising from the use of any information it contains.

ROYAL SOCIETY OF CHEMISTRY

www.rsc.org/methods

Effect of the tip length of multi-branched AuNFs on the detection performance of immunochromatographic assays

Peng Xu[ab], Juan Li[ab], Xiaolin Huang[ab], Hong Duan[ab], Yanwei Ji[ab], Yonghua Xiong*[ab]

[a] State Key Laboratory of Food Science and Technology, Nanchang University, 235 Nanjing East Road, Nanchang 330047, P. R. China.

[b] Jiangxi-OAI Joint Research Institute, Nanchang University, 235 Nanjing East Road, Nanchang 330047, P. R. China.

*Correspondence to:

Dr. Yonghua Xiong

State Key Laboratory of Food Science and Technology, and Jiangxi-OAI Joint Research Institute, Nanchang University.

Address: 235 Nanjing East Road, Nanchang 330047, P. R. China.

Phone: +0086-791-8833-4578. Fax: +0086-791-8833-3708.

E-mail: yhxiongchen@163.com.

ABSTRACT

The traditional immunochromatographic assay (ICA) using conventional spherical gold nanoparticles (AuNSs, 30–40 nm) as labeled probes usually suffers from low sensitivity because of insufficient probe optical intensity. Previously, we demonstrated that larger gold nanoflowers (AuNFs, 75 nm) possessed higher optical brightness can greatly improve ICA sensitivity over conventional AuNSs. However, the improve mechanism which resulted from either larger diameter or longer tips or both is not clear. To elaborate the influence of tip length on the sensitivity of ICA while put particle size aside temporarily, herein, three types of gold nanoparticles (AuNPs) with similar diameter in the range of 30–40 nm, including conventional AuNSs (no tip), short-tip AuNFs (tip length, 7–8 nm), and long-tip AuNFs (tip length, 13–15 nm), were synthesized. Results showed that long-tip AuNFs as labeled probes exhibited the highest signal enhancement in ICA because of the strongest optical absorbance and highest affinity to the sample. The cut-off limit (for visual qualitative detection), half maximum inhibitory concentration, and detection limit (for quantitative analysis) of long-tip AuNF-based strip were 2, 0.61, and 0.07 ng/mL which are 2.5, 2.75, and 4.14 times lower than those of AuNS-based strips, respectively. Additionally, taking into account the cost, only 20% of AuNFs and antibody consumption for each strip using long-tip AuNFs as labeled probe compared to AuNSs which significantly reduce manufacturing costs in the large-scale production. Obviously, long-tip AuNFs show great application potential as an alternative to traditional AuNSs in the ICA platform.

Keywords: immunochromatographic assay; multi-branched gold nanoflowers; tip length; detection performance.

1. Introduction

Immunochromatographic assay (ICA) is one of the most prevalent points of care testing formats because of its unique advantages over laboratory-based testing, these advantages include simplicity, rapidity, low cost, and acceptable selectivity and precision.[1] Various colloid gold nanoparticle (AuNP)-based ICA products are widely used for on-site screening detection of biomarkers, drugs, chemical contamination, bio-toxins, and pathogens in clinical diagnosis, food safety, and environment monitoring. However, conventional AuNP-based ICA usually suffers from relative low sensitivity because of the insufficient optical density of the probe.[2] As such, many novel nanoparticles (NPs), including luminescent (e.g., quantum dots, up-converting phosphor NPs, and dye-doped NPs)[3–6] and magnetic NPs,[7] have been introduced as alternative labels to improve the analytical sensitivity of ICA because of their strong fluorescent and magnetic properties. Colored NPs, such as colloidal carbon,[8] colloidal selenium, as well as colloidal iron oxide NPs, have also been used to enhance the sensitivity of ICA because of their high signal-to-noise ratio or signal intensity.[9,10] Several AuNP-based signal enhancement strategies, such as AuNP-modified nanomaterials and dual AuNP-based signal enhancements, have been reported to achieve high sensitivity in ICA.[11,12]

Although various novel NPs and signal amplified strategies have been successfully applied to enhance the performance of traditional ICA, spherical AuNPs (AuNSs) with diameters of 30–40 nm are the most commonly labeled NPs because of its low cost, good biocompatibility, as well as ease of preparation and bio-conjugation.

Compared with AuNSs, multi-branched gold nanoflowers (AuNFs) exhibit more unique optical characteristics, such as stronger surface-enhanced Raman scattering and higher extinction coefficients, because its tips and core–tip interactions act as an antenna to produce electromagnetic field enhancements.[13–16] For example, Zhang et al. used 280 nm AuNFs as probes to enhance the sensitivity of sandwich ICA, and achieved a 10^3 cfu/mL detection limit for *Escherichia coli* O157:H7 because the large surface-to-volume ratio of the AuNFs improves the antibody amounts of immobilization.[17] Previously, our group also used 75 nm multi-branched AuNFs to develop a competitive ICA for the quantitative detection of aflatoxin B_1 with a half maximal inhibitory concentration (IC_{50}) at 4.17 pg/mL; this value is 10 times lower than those of AuNS (20 nm)-based ICA systems.[18] The above results confirmed that the AuNFs with larger sizes are beneficial in improving ICA sensitivity.

The optical intensity of AuNFs is not only associated with the morphology of the AuNFs but also their size. However, a comprehensive study of the tip length of AuNFs on the detection performances of ICA has yet to be published. To elaborate the enhancing mechanism of AuNF tip length on the sensitivity of ICA further, we synthesized three types of AuNPs with average diameters of 30–40 nm, including conventional AuNSs (no tip), short-tip AuNFs (tip length, 7–8 nm), and long-tip AuNFs (the tip length 13–15 nm), as labeled probes. Ochratoxin A (OTA), a secondary metabolite mainly produced by several fungi of the *Aspergillus* and *Penicillium* families, was chosen as the model analyte because it is one of the priority mycotoxin contaminants in agricultural products, such as grains, cereals, nuts, beans,

and maize.[19–21] Three types of AuNPs with different tip lengths were used as labeled probes to prepare strips, and the effect of the tip length of these AuNPs on the detection performance of ICA was evaluated in terms of several aspects; these aspects include the binding kinetics between the probes and OTA-labeled bovine serum albumin (OTA-BSA) conjugates on the test line and donkey anti-mouse antibodies on the control line; consumption of AuNPs and antibodies for each strip; the cut-off limit of the strips by the naked eye; IC_{50}, detection limit (LOD) for quantitative analysis, and the quantitative interpretation time.

2. Materials and methods

2.1 Chemicals and materials

OTA, hydrogen tetrachloroaurate (III) hydrate ($HAuCl_4 \cdot 3H_2O$), trisodium citrate ($Na_3C_6H_5O_7 \cdot 12H_2O$), hydroquinone, and BSA were purchased from Sigma–Aldrich (St. Louis, MO, USA). A sample pad, conjugate pad, nitrocellulose (NC) membrane, and absorbent pad were obtained from Schleicher and Schuell GmbH (Dassel, Germany). The OTA labeled BSA conjugates (OTA-BSA, molar ratio of 10:1) and ascitic fluids containing anti-OTA monoclonal antibody (mAb) were provided by Wuxi Zodoboer Biotech. Co., Ltd. (Wuxi, China). All other inorganic chemicals and organic solvents used in this work were of analytical reagent grade or better. The water used throughout the experiments was distilled and purified by a Milli-Q system (Millipore, Milford, MA, USA). The BioDot XYZ platform combined with a motion controller, BioJet Quanti3000k dispenser, and AirJet Quanti3000k dispenser for solution dispensing was supplied by BioDot (Irvine, CA, USA).

2.2 Synthesis of AuNSs and multi-branched AuNFs

AuNSs with average diameters of 20 and 33 nm were prepared following a method previously reported with slight modifications.[22] Briefly, a flask containing 100 mL of 0.01% (w/v) $HAuCl_4$ solution was heated to boiling under vigorous stirring and then rapidly combined with 2.7 mL of 1% trisodium citrate solution. The solution was kept boiling for another 15 min. The color of the solution changed to a deep red, indicating the formation of 20 nm AuNSs. The 33 nm AuNSs were prepared by adding 1.35 mL of trisodium citrate solution. The as-prepared AuNS solutions were cooled to ambient

temperature and then stored at 4 °C prior to use. The concentrations of AuNSs with average diameters of 20 nm and 33 nm were calculated at 1.17 nmol/L and 170 pmol/L according to the method proposed by Haiss et al.[23]

Multi-branched AuNFs with short or long tips were synthesized through a seeding growth approach according to a previously reported method[24,25] with some modifications (shown in Scheme 1). Short-tip (35 nm) AuNFs were prepared as follows: 375 μL of 1% (w/v) $HAuCl_4$, 220 μL of 1% trisodium citrate, and 2.5 mL of as-prepared 20 nm AuNS seed solutions were added to 100 mL of pure water under vigorous stirring. Subsequently, 1 mL of 30 mmol/L hydroquinone solution was added to this mixture. The reaction mixture was maintained at room temperature for 30 min with constant stirring and then centrifuged at 9000 *g* for 10 min. The pellets were re-dissolved with 59 mL of 0.02% trisodium citrate solution.

To prepare long-tip (36 nm) AuNFs, the contents of the AuNS seed solution were reduced to 2.0 mL, while other parameters were maintained consistent with the above experimental conditions. After centrifugation at 9000 *g* for 10 min, the precipitate was re-dissolved with 47 mL of 0.02% trisodium citrate solution. The final concentrations of the both of as-prepared AuNF solutions were calculated at 50 pmol/L based on the content of their AuNS seeds.

The morphology and size distribution of AuNSs and multi-branched AuNFs were characterized by high-resolution transmission electron microscopy (TEM, JEOL JEM 2100, Tokyo, Japan). The maximum surface plasmon resonance (SPR) peaks of the

above AuNPs were determined by double-beam UV-visible spectrophotometer (Cintra10e; GBC, Victoria, Australia).

2.3 Preparation of AuNS and AuNF probes

Anti-OTA ascitic fluids were used to label AuNSs and AuNFs directly according to the method of Yokota et al.[26] The as-prepared 33 nm AuNS solution (170 pmol/L) was diluted with 0.02% (w/v) trisodium citrate solution to a final concentration of 50 pmol/L. The pH of the diluted AuNS, short, and long-tip AuNF solutions was adjusted to 7.0 with 0.2 mol/L K_2CO_3. To prepare AuNS, short, and long-tip AuNF probes, 100 μL of anti-OTA ascitic fluids (0.45 mg/mL) was added dropwise to 10 mL of each of the AuNP solutions (50 pmol/L) at room temperature with gentle stirring. The obtained AuNS (AuNS-mAbs) and multi-branched AuNF (AuNF-mAbs) probes were then blocked with 1 mL of 10% (w/v) BSA solution for another 60 min. After centrifugation at 8000 *g* for 10 min to remove unbound ascitic fluids, the three probes were dissolved with 500 μL of phosphate buffered saline (PBS) containing 5% sucrose, 2% trehalose, 1% PEG 20,000, 1% BSA, and 0.25% Tween-20. The final concentration of AuNPs of the three obtained probes was 1 nmol/L, and the consumption of anti-OTA ascitic fluids per nmol probe was 9×10^4 μg .

2.4 Immunological kinetic analysis of the strip

An immuno-dynamic process between the probes and antigen interaction (OTA-BSA on the T line and donkey anti-mouse IgG on the C line) on the strip was performed according to our previous report.[18] In brief, 2 μL of AuNS or AuNF probes (1 nmol/L) was premixed with 80 μL of PBS, and then the mixture was pipetted into a sample

well. After running for 1 min, the strip was inserted into a commercial HG-8 strip reader (Shanghai Huguo Science Instrument Co., Ltd., Shanghai, China). The optical densities on the test (OD_T) and control (OD_C) lines, as well as the ratio of OD_T/OD_C (T/C), were recorded every 30 s for 60 min. Kinetic curves between the probes and OTA-BSA, as well as between the probes and donkey anti-mouse IgG, were established by plotting the OD_T, OD_C, and T/C values against time.

2.5 Preparation of AuNS and multi-branched AuNF based strips

The strips were prepared as our previous report with slight modifications.[18] As shown in Scheme 1, the test strip comprised five parts, including the sample pads, conjugate pads, absorbent pads, an NC membrane, and polyvinyl chloride backing. The sample pad was soaked in 0.1 M PBS (pH 7.4) solution containing 0.1% BSA, 0.4% Tween-20, and 0.05% sodium azide and then dried at 60 °C for 4 h. The conjugate pad was pretreated with 0.01 M PBS (pH 7.4) solution containing 0.2% Tween-20 and 2% sucrose at 60 °C for 4 h. The OTA-BSA conjugate (1.2 mg/mL) and donkey anti-mouse IgG (0.4 mg/mL) were sprayed on the NC membrane as the test (T) and control (C) lines with a dispensing density of 0.75 μL/cm. The distance between the T and C lines was 5 mm. The NC membrane was then dried at 37 °C for 12 h. AuNS-mAbs were jetted onto the conjugate pad at a density of 4 μL/cm. To produce the same signal intensity with the AuNS-based strip on the T line, the dispensation rates of multi-branched AuNF with short and long tips were set to 2.0 μL/cm and 0.8 μL/cm, respectively. The as-prepared conjugate pads were then dried at 37 °C for 3 h with a vacuum dryer. The NC membrane, conjugate pad, sample pad, and

absorbent pad were laminated and pasted onto a PVC backing and then cut into 4 mm wide strips. All of the strips were inserted into rigid plastic cassettes, packaged in a plastic bag containing a desiccant gel, and stored at room temperature until use.

2.6 Performance comparison between AuNS and AuNF based strip

The effects of AuNP tip lengths on the performance of the AuNP based-strips were evaluated. The performance of the three strips was compared in terms of consumption of AuNPs and anti-OTA ascitic fluids for each strip, as well as the cut-off limits for qualitative detection. The interpretation time, IC_{50}, and LOD of the strip for quantitative analysis were also evaluated. The AuNP contents of each strip can be calculated via the following equation: $N_{Au}=C_{probes} \times V \times W$, where N_{Au} is the mole quality of AuNPs on each strip (nmol), V is the dispensation rate of AuNP probe sprayed on the conjugated pad (μL/cm), and C_{probes} and W are two constants representing the concentration of AuNP probes (1×10^{-6} nmol/μL) and the width of each strip (0.4 cm), respectively. The consumption of anti-OTA ascitic fluids for each strip could be calculated as $N_{Au} \times 9 \times 10^4$ (μg). The cut-off limit was defined as the minimum concentration of OTA that causes no color on the test line. The quantitative curves of the strips were established by plotting the competitive inhibition rate ($1–B/B_0$) against the logarithm of the OTA concentrations according to our previous report,[18] where B_0 and B represent the ratio of T/C of the negative sample and an OTA-spiked PBS buffer containing 10% methanol, respectively. The regression equation was described by a logistic four-parameter equation. The LOD of the strip

was defined as 10% OTA competitive inhibition concentration. The IC_{50} value was obtained from five independent experiments.

3. Results and discussion

3.1 Synthesis and Characterization of AuNSs and AuNFs

In the present study, the AuNSs were synthesized according to a citrate reduction method. The obtained AuNS solution appeared red. The TEM image in Fig. 1A reveals a relatively uniform sphere with an average diameter of 33 ± 2 nm (n = 50). The AuNFs with different tip lengths were synthesized using a seeding growth approach. The diameters of the resultant AuNFs were adjusted by changing the concentrations of hydroquinone, $HAuCl_4$, and sodium citrate in the reaction, and the tip lengths of the AuNFs were regulated by adding different amounts of AuNS seeds (20 nm). Increasing amounts of AuNS seeds would supply fewer gold atom epitaxial depositions for each AuNS seed, resulting in short-tip growth.[24] Fig. 1B and 1C demonstrate that the two kinds of as-synthesized AuNFs are purple and blue, respectively. The TEM image in Fig. 1B shows flower-like AuNPs with a solid core and several short tips with an average length of 7–8 nm. The TEM image of the AuNFs in Fig. 1C exhibits a solid core with some long tips (13–15 nm). The size distributions of the short- and long-tip AuNFs were determined to be 35 ± 2 nm and 36 ± 2 nm, respectively, by calculating the average diameter of 50 gold particles in the TEM images. The UV-vis spectra in Fig. 1D demonstrate that the maximum SPR peak of the as-prepared AuNSs is 527 nm (red), whereas those of the short and long tip AuNFs exhibit maximum absorption peaks of SPR at 575 nm (purple) and 605 nm (blue), respectively, which is consistent with the optical color observed. The absorbances of the short and long tip AuNFs in Fig. 1D were 2.5 and 4 times more

than that of the conventional AuNSs at the same particle's concentration (50 pmol/L). Under the same concentration, the higher absorbance means the higher extinction coefficient because the OD value of target analyte can be calculated via the following equation: $A=\varepsilon \cdot C \cdot L$, according to Lambert-Beer equation, where A is the absorbance of target analyte, ε is the extinction coefficient, C is the concentration of target analyte and L is the thickness of the liquid layer, respectively. Moreover, the three AuNP solutions were stored at room temperature for 60 d to evaluate their colloidal stability. All three types of AuNPs exhibited no flocculation or aggregation and could maintain a good colloidal stability in solution even after 2 months of storage.

3.2 Preparation and characterization of AuNS and AuNF probes

The surface chemistry properties of the AuNSs/AuNFs and the pH of the reaction buffers are two important factors influencing antibody adsorption and bioactivity.[27] To obtain ligand properties identical to those of the as-prepared AuNSs, the hydroquinone on the surface of short- or long-tip AuNFs was replaced by re-dissolving the AuNFs in 0.02% trisodium citrate solution. The AuNSs and AuNFs with citrate as the ligand were directly labeled with the anti-OTA ascitic fluids. The optimal label pH of anti-OTA ascitics for AuNSs and AuNFs were determined by adding different volumes of 0.2 mol/L K_2CO_3 to a final pH of 6.5–9.0. The labeling efficiency and bioactivity of the AuNSs and AuNFs for the anti-OTA ascitic fluids were evaluated by recording the OD_T value after running the same amounts of AuNS or AuNF probes on the strips. Fig. 2A indicates that the optimized pH values for ascitic fluids labeling on AuNSs, short-tip, and long-tip AuNFs were 7.0. The

maximum SPR peaks of AuNS, short-tip, and long-tip AuNF probes red-shifted by 4, 6, and 12 nm, respectively (Fig. 1D), indicating that the anti-OTA ascitic fluids were successfully coupled on the surface of three kinds of AuNPs. Moreover, the saturated labeled amounts of anti-OTA ascitic fluids on three kinds of AuNPs were optimized by dropping 2.25, 4.5, 9.0, 13.5, 18, and 22.5 μg of anti-OTA ascitic fluids to 1 mL of pH adjusted AuNS and AuNF solutions (50 pmol/L). Fig. 2B indicates that the OD_T value of the strip increases sharply with increasing ascitic fluids amount from 2.25 μg to 4.5 μg and then slowly declines with further increases in ascitic fluids amount. We speculate that the steric hindrance would lead to the low binding bioactivity of the mAbs to OTA antigen on the test line when an excessive density of the mAbs is on the surface of the AuNSs. Thus, the saturated labeled amounts of anti-OTA ascitic fluids on conventional AuNSs were 4.5 μg per mL of AuNS solution. For the short- and long-tip AuNFs, changes in OD_T exhibited the same trend at low amounts of ascitic fluids ranging from 2.25 μg to 22.5 μg. When the labeled ascitic fluids amounts were further increased, the OD_T continued to slowly ascend and then reached a maximum value. Fig. 2B indicates that the saturated labeled amounts of anti-OTA ascitic fluids on the short- and long-tip AuNFs were 9.0 μg and 13.5 μg per mL AuNF solution, respectively. Long-tip AuNFs possess a higher protein loading capacity compared with conventional AuNSs and short-tip AuNFs because of their complex three-dimensional structure and large surface area. To eliminate the influence of antibody amounts on the surface of AuNPs on the immuno-reaction of the strip, AuNS and two AuNF probes were prepared by labeling the same amounts of anti-OTA

ascitic fluids (4.5 μg) with 1 mL of AuNS or AuNF solutions (50 pmol/L) in subsequent experiments.

3.3 Immunological kinetics analysis of the ICA

The development of OD values of the strip can indirectly reflect the antibody-antigen dynamic interactions between the AuNP probes and OTA-BSA antigen (on the T line) or donkey anti-mouse IgG (on the C line) of the strips. To elaborate the length of tips of AuNPs on the signal intensity and affinity of the probe, two kinds of AuNF and one AuNS probes were used to run strips at the same experiment conditions, including 2 μL of probes (1 nmol/L), 1.2 mg/mL of OTA-BSA on the T line and 0.4 mg/mL of donkey anti-mouse IgG on the C line. The results of immunological kinetics analysis of the strips are shown in Fig. 3A. In the AuNS-based strip, the signal intensities on the T and C lines increased with the increase of immuno-reaction time, and then reached an immuno-dynamic balance after 26 min (ODs achieved a constant intensity). The maximum ODs on the T and C lines were 430 ± 8 and 667 ± 6, respectively. For the short-tip AuNF-based strip, the immuno-dynamic balance time (22 min) was slightly less than that of the AuNS-based strip. The maximum ODs on the T and C lines were 1156 ± 19 and 1231 ± 17, respectively, which are 2.69 and 1.85 times higher than that of the AuNS-based strip. For the long-tip AuNF-based strip, the maximum OD_T and OD_C values were 1736 ± 10 and 1349 ± 8, respectively, which are 4.04 and 2.02 times higher than that of the AuNS-based strip. The immuno-dynamic balance time for long-tip AuNF-based strip is 15 min. The above results indicated that long-tip AuNF-mAb probes possessed the strongest signal

intensity (approximately four fold signal enhancement on the T line) and the highest antibody-antigen dynamic efficiency because of its short balance time (15 min). In general, probes with a high affinity to the antigen on the T line or with a quicker migration rate on the NC membrane would produce a quicker immuno-dynamic reaction for strip assay. In theory, high-affinity probes could produce a higher T/C values because the probes are more easily captured by the antigen on the strip, whereas the probes with a quicker migration rate should not affect T/C values.[21,28] Fig. 2B shows that the T/C ratio of AuNF-based strip is remarkably higher than of AuNS-based strip (T/C = 0.67 ± 0.03), and long-tip AuNF-based strip exhibited the highest T/C value at 1.29 ± 0.02. The stereogram of the strips displayed in the inset of Fig. 2B indicates that the visual color of the AuNS-based strip on the T line is significantly weaker than that on control line; the opposite results were observed for the long-tip AuNF-based strip. These results demonstrated that the long-tip AuNF-mAbs possess a higher affinity to OTA-BSA on the T line compared with other two kinds of AuNP-mAb probes, suggesting that the complicated three-dimensional structure of the long-tip AuNF could make antibody more exposure and stretch. Thus, the long-tip AuNF as probes for the strip assay are involved in two signal enhance mechanisms, including excellent optical property and higher affinity to detection antigen.

3.4 Performance comparison between AuNS and AuNF based strip

AuNF-mAbs as labeled probes could significantly enhance signal intensity of T and C lines. Theoretically, fewer AuNF-mAbs could achieve the same absorbance as

AuNS-mAbs in the strip test, which is beneficial to the sensitivity of competitive ICA.[29] To verify whether the AuNFs could improve the sensitivity of the ICA, three types of strips were prepared by using AuNS-mAbs, short-tip AuNF-mAbs, and long-tip AuNF-mAbs as labeled probes. The OD_T values of the three strips were controlled at the same level to detect OTA-free samples. For the competitive immunoassay, the amount of AuNP-mAbs and the concentration of OTA-BSA were considered the most important parameters controlling the sensitivity of the strip and the OD_T value on the T line in negative samples. First, the parameters of AuNS-based strip were optimized by a similar "checkerboard titration" method with different AuNS-mAbs contents under a series of BSA-OTA conjugates on the T line for various combinations.[30] As we know, the ODs of the strip on the both lines for negative sample and the competitive inhibition rates for positive sample were considered as the two important factors to evaluate the performance of the strip. As shown in table 1, the competitive inhibition ratio of the No. 7 combination is the best, but its OD value on the test line is too weak (OD_T=171.1). For No. 1 combination, two visual clear bands were observed on both lines for detection of negative samples, and the means of OD_T and OD_C of are 314 and 302, respectively, whereas the competitive inhibition rate of the 2 ng/mL OTA-spiked sample was achieved at 65.7%. Thus, the No 1 combination was considered as the optimal conditions with 4 μL/cm dispensation rate of AuNS-mAbs on the conjugation pad and 1.2 mg/mL BSA-OTA on the T line, respectively. To prepare the two other types of AuNF-based strips, the concentration of AuNF-mAb probes and the content of BSA-OTA antigen on the T line were

consistent with those of AuNS based strip; the absorbance on the test line was controlled by changing the jetted volumes (μL/cm) of the short- or long-tip AuNF–mAb probes on the conjugate pads. The results showed that 2.0 μL/cm of short-tip AuNF probes and 0.8 μL/cm of long-tip AuNF probes are sufficient to achieve the nearly same signal intensities on the T line for short-tip AuNF-based strip (OD_T = 307) and long-tip AuNF-based strip (OD_T = 311), respectively. Then, the cut-off limits of three kinds of strips for visual qualitative detection were determined. The Fig. 4D indicates that the cut-off limit of AuNS-based strip was 5 ng/mL, whereas those of the short- and long-tip AuNF-based strips were 3 and 2 ng/mL, respectively. The quantitative performances of the three types of strips including the interpretation time, IC_{50}, and LOD, were also evaluated. As shown in Fig. 3B, the constant T/C values of AuNS-, short-tip AuNF-, and long-tip AuNF-based strips were observed after 17, 15, and 12 min, respectively. Thus, the interpretation times of AuNS-, short-tip AuNF-, and long-tip AuNF-based strips for quantitative analysis were 17, 15, and 12 min, respectively. Long-tip AuNFs as labeled probes showed a higher immunological kinetic efficiency, and therefore, were more suited for on-site detection in food safety monitoring. The quantitative standard curves of three kinds of strips for OTA detection were described by a logistic four-parameter equation (Fig. 4A, 4B, and 4C). The regression equation of AuNS-based strip is $y = 145.6914/[1 + (x/2.9255)^{-1.0554}]-1.8735$ (R^2 = 0.9903), where y is the competitive inhibition rate $(1-B/B_0) \times 100\%$ and x is the OTA concentrations from 0 ng/mL to 5 ng/mL. The IC_{50} of AuNS-based strip was 1.68 ng/mL (n = 5), and the LOD was 0.29 ng/mL according

to a 10% OTA competitive concentration. The IC_{50} values of the short-tip AuNF- and long-tip AuNF-based strip were calculated using their regression equations as 0.84 and 0.61 ng/mL, and the LOD values were 0.10 and 0.07 ng/mL, respectively. The above results indicated that long-tip AuNFs exhibited the most significant advantages in improving sensitivity, as well as the immunological kinetic efficiency of the strip. These distinctive advantages of long-tip AuNFs as labeled probes in ICA can be attributed to two aspects including their higher molar extinction coefficient and higher affinity as labeled probes. In addition, cost is also an important consideration for strip production. In the present study, the amounts of long-tip AuNFs and anti-OTA ascitic fluids for each strip were 0.32 fmol and 0.29 μg, which is only 20% consumption of conventional AuNS-based strips. Thus, using long-tip AuNFs as an alternative to conventional AuNSs for labeled probes require lower costs for large-scale strip production.[31,32]

4. Conclusions

In this work, we demonstrated that the morphology of AuNPs can significantly influence the detection performance of ICA. Long-tip AuNFs as labeled probes in ICA show improved performance in sensitivity and immunological kinetic efficiency compared with the ICA based on conventional AuNSs as labels. The cut-off limit of the long-tip AuNF-based strip for visual inspection reached 2 ng/mL, which is 2.5-fold lower than that of conventional AuNS-based strip. The IC_{50} and LOD of the long-tip AuNF-based strip are also 2.75, and 4.14 times lower than those of the conventional AuNS-based strip. In addition, the consumption of the AuNPs and antibodies for each long-tip AuNF-based strip are only 20% of the AuNS-based strip, which helps reduce the manufacturing costs of large-scale strip production. In summary, long-tip AuNFs exhibit significant application potential as an alternative to traditional AuNSs for labeled probes in the ICA platform.

Acknowledgements

This work was supported in part by the National Basic Research Program of China (2013CB127804), the National Natural Science Foundation of China (31271863), Training Plan for the Main Subject of Academic Leaders of Jiangxi Province (20142BCB22004).

References

(1) K. Meng, W. Sun, P. Zhao, B. B. Dzantiev, N. A. Byzova, A. E. Urusov and A. V. Zherdev, *Trends Anal. Chem.*, 2014, **55**, 81–93.

(2) K. Omidfar, F. Khorsand and M. D. Azizi, *Biosens. Bioelectron.*, 2013, **43**, 336–347.

(3) A. N. Berlina, N. A. Taranova, A. V. Zherdev, M. N. Sankov, I. V. Andreev, A. I. Martynov and B. B. Dzantiev, *Plos One.*, 2013, **8**, 1–8.

(4) P. Zhao, Y. Wu, Y. Zhu, X. Yang, X. Jiang, J. Xiao, Y. Zhang and C. Li, *Nanoscale*, 2014, **6**, 3804–3809.

(5) X. Huang, Z. P. Aguilar, H. Li, W. Lai, H. Wei, H. Xu and Y. Xiong, *Anal. Chem.*, 2013, **85**, 5120–5128.

(6) C. Liu, Q. Jia, C. Yang, R. Qiao, L. Jing, L. B. C, Wang, L. Xu and M. Gao, *Anal.Chem.*, 2011, **83**, 6778–6784.

(7) M. Ren, H. Xu, X. Huang, M. Kuang, Y. Xiong, H. Xu, Y. Xu, H. Chen and A. Wang, *Appl. Mater. Interfaces*, 2014, **6**, 14215–14222.

(8) C. S. Pantaleon, J. Wichers, A. A. Somovilla, A. V. Amerongen and A. A. Fuentes, *Biosens. Bioelectron.*, 2013, **42**, 170–176.

(9) I. Y. Goryacheva, P. Lenain and D. S. Saeger, *Trends Anal. Chem.*, 2013, **46**, 30–43.

(10) W. Yang, X. Li, G. Liu, B. Zhang, Y. Zhang, T. Kong, J. Tang, D. Li and Z. Wang, *Biosens. Bioelectron.*, 2011, **15**, 3710–3713.

(11) D. Tang, J. C. Sauceda, Z. Lin, O. E. Basova, I. Goryacheva, S. Biselli, J. Lin and

D. K. Niessner, *Biosens. Bioelectron.*, 2009, **25**, 514–518.

(12) J. Zhu, N. Zou, D. Zhu, J. Wang, Q. Jin, J. Zhao and H. Mao, *Clin. Chem.*, 2011, **57**, 1732–1738.

(13) F. Hao, C. L. Nehl, J. H. Hafner and P. Nordlander, *Nano Lett.*, 2007, **3**, 729–732.

(14) C. L. Nehl, H. Liao and J. H. Hafner, *Nano Lett.*, 2006, **4**, 683–688.

(15) S. K. Dondapati, T. K. Sau, C. Hrelescu, T. A. Klar, F. D. Stefani and J. Feldmann, *ACS Nano*, 2010, **11**, 6318–6322.

(16) A. G. Martinez, S. Barbosa, I. S. Santos and L. M. L. Marzan, *Curr. Opin. Colloid Interface Sci*, 2011, **16**, 118–127.

(17) L. Zhang, Y. Huang, J. Wang, Y. Rong, W. Lai, J. Zhang and T. Chen, Langmuir., 2015, **31**, 5537–5544.

(18) Y. Ji, M. Ren, Y. Li, Z. Huang, M. Shu, H. Yang, Y. Xiong and Y. Xu, *Talanta*, 2015, **142**, 206–212.

(19) A. E. Urusov, S. N. Kostenko, P. G. Sveshnikov, A. V. Zherdev and B. B. Dzantiev, *J. Anal. Chem.*, 2011, **66**, 770–776.

(20) X. Liu, Y. Xu, D. Wan, Y. Xiong, Z. He, X. Wang, S. J. Gee, D. Ryu and B. D. Hammock, *Anal. Chem.*, 2015, **87**, 1387–1394.

(21) C. Giovannoli, C. Passini, F. D. Nardo, L. Anfossi and C. Baggiani, *J. Agric. Food. Chem.*, 2014, **62**, 5220–5225.

(22) G. Frens, *Nature*, 1973, **241**, 20.

(23) W. Haiss, N. T. K. Thanh, J. Aveyard and D. G. Fernig, *Anal. Chem.*, 2007, **11**, 4215–4221.

(24) J. Li, J. Wu, X. Zhang, Y. Liu, D. Zhou, H. Sun, H. Zhang and B. Yang, *J. Phys. Chem. C*, 2011, **115**, 3630–3637.

(25) S. D. Perrault and W. C. W. Chan, *J. Am. Chem. Soc.*, 2009, **47**, 17042–17043.

(26) T. Yokota, D. E. Milenic, M. Whitlow and J. Schlom, *Cancer Res.*, 1992, **52**, 3402–3408.

(27) S. Thobhani, S. Attree, R. Boyd, N. Kumarswami and J. Noble, *J.Immunol. Methods*, 2010, **356**, 60–69.

(28) J. Xie, Q. Zhang, J. Y. Lee and D. I. Wang, *ACS Nano*, 2008, **12**, 2473–2480.

(29) B. B. Dzantiev, N. A. Byzova, A. E. Urusov and A. V. Zherdev, *Trends Anal. Chem.*, 2014, **55**, 81–93.

(30) W. Xu, X. Chen, X. Huang, W. Yang, C. Liu, W. Lai, H. Xu and Y. Xiong, *Talanta*, 2013, **114**, 160–166.

(31) S. Song, N. Liu, Z. Zhao, E. N. Ediage, S. Wu, C. Sun, S. D. Saeger and A. Wu, *Anal. Chem.*, 2014, **86**, 4995–5001.

(32) D. Zhang, P. Li, Q. Zhang and W. Zhang, *Biosens. Bioelectron.*, 2011, **26**, 2877–2882.

451 **Table**

452 **Table 1.** Optimization of the parameters of the AuNS-based strip[#].

No	The dispensation rate of AuNS-mAbs on the conjugation pad (μL/cm)	The concentration of OTA-BSA on the test line (mg/mL)	OD value on the test line	OD value on the control line	The competitive inhibition ratios, $(1-B/B_0) \times 100\%$
1*	4.0	1.2	314	301.9	65.7
2	5.0	1.0	305.2	505.2	43.5
3	6.0	0.8	221.7	344.3	54.3
4	4.0	1.0	274.6	415.1	58.7
5	5.0	0.8	197.5	388.7	54.7
6	6.0	1.2	428.6	502.2	54.5
7	4.0	0.8	171.1	357.0	79.6
8	5.0	1.2	339.3	407.3	40.9
9	6.0	1.0	325.2	494.3	56.9

453 Notice: [#] The labeled amounts of anti-OTA ascitic fluids per mL AuNS solution (50

454 pmoL/L) was 4.5 μg; * The optimal combinations.

455

Figure Captions

Scheme 1. Schematic demonstration of the length of tips of AuNFs on the detection performance of immunochromatographic assay.

Figure 1. Characterization of AuNSs and AuNFs. A–C: TEM images of AuNSs, short-tip AuNFs, and long-tip AuNFs. Inset: Corresponding single particle images and photographic images of the as-synthesized AuNP solution; D: UV-visible spectra of the three types of AuNPs (solid line) and AuNP-mAb probes (dash line).

Figure 2. Preparation and characterization of AuNS and AuNF probes. A: Optimization of labeling pH of anti-OTA ascitic fluids on AuNSs and AuNFs ; B: Optimized saturated labeled amounts of anti-OTA ascitic fluids on AuNSs and AuNFs.

Figure 3. Immunological kinetics analysis of the ICA strips. A: Immunoreaction dynamics of OD_T and OD_C of AuNSs, short-tip AuNFs, and long-tip AuNFs against immunoreaction time; B: Immunoreaction dynamics of the ratio of T/C of AuNSs, short-tip AuNFs, and long-tip AuNFs against immunoreaction time; Inset: stereogram of the strips with 2 μL of AuNS-mAb, short-tip AuNF-mAb, and long-tip AuNF-mAb probes (1 nmol/L).

Figure 4. Calibration curves of strips for different concentrations of OTA. A: spherical AuNPs based strip; B: short-tip AuNFs based strip; C: long-tip based strip; D: the stereograms of three types of strips.

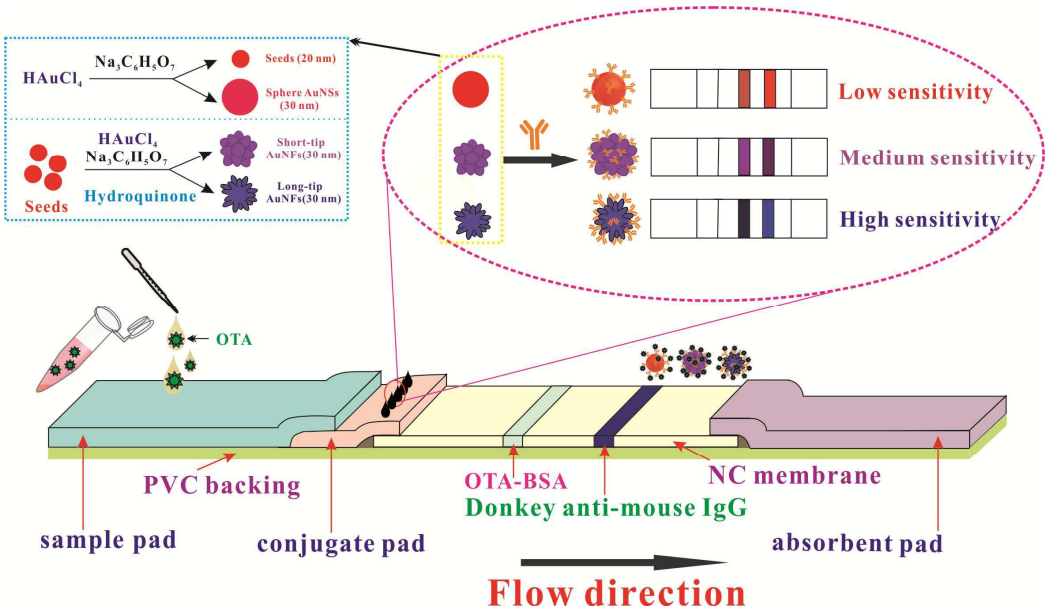

Scheme 1. Xu *et al.*

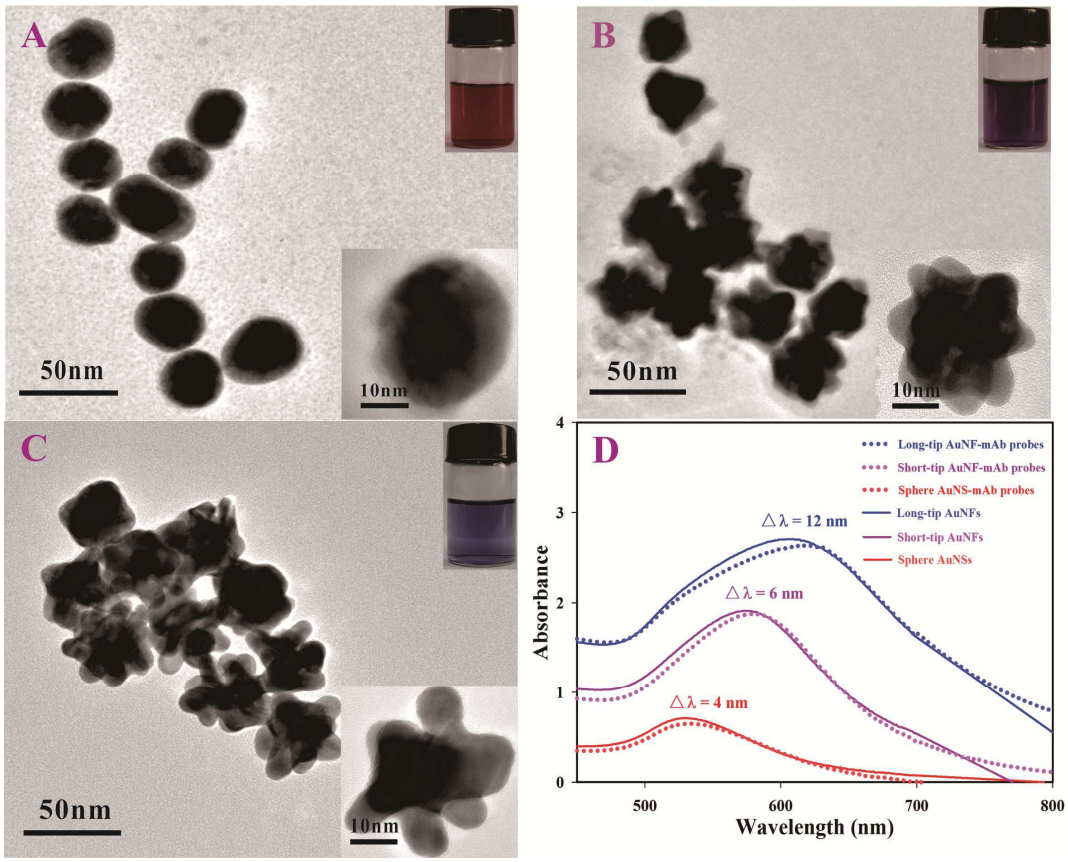

Figure 1. Xu *et al*.

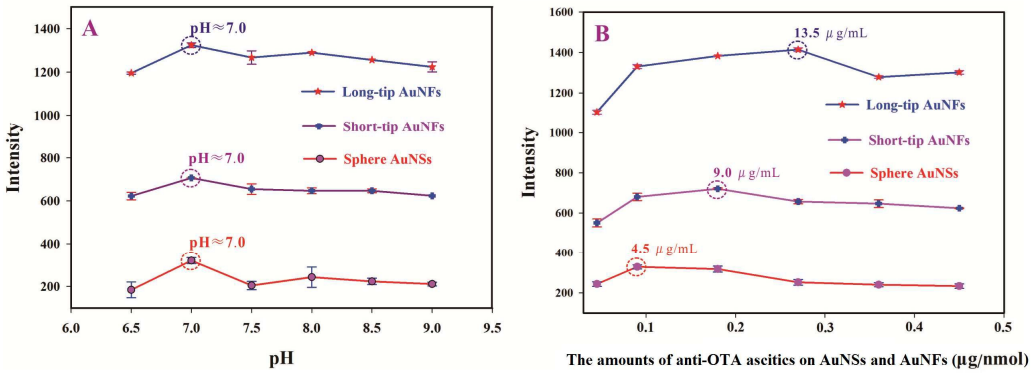

Figure 2. Xu *et al*.

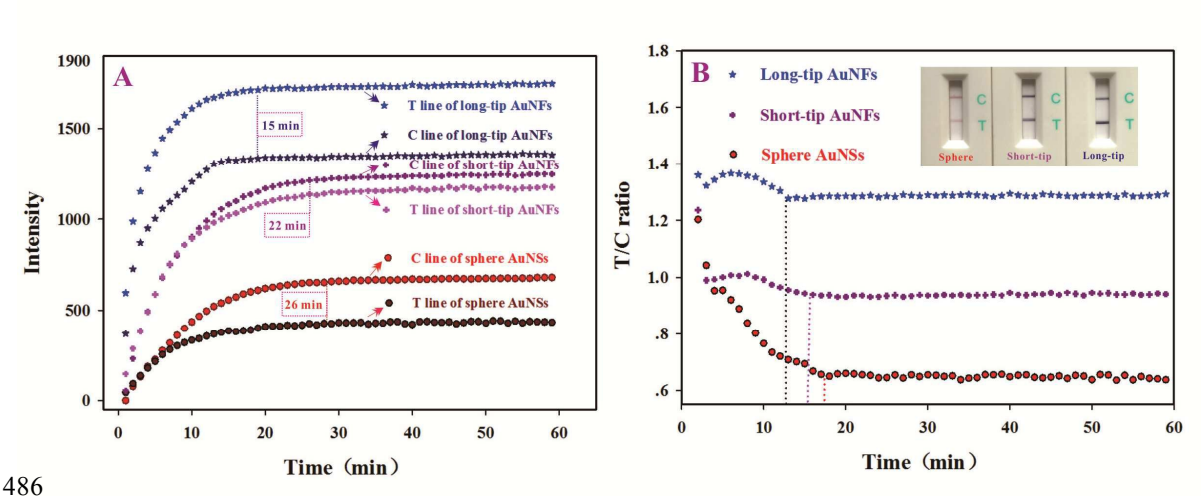

Figure 3. Xu *et al*.

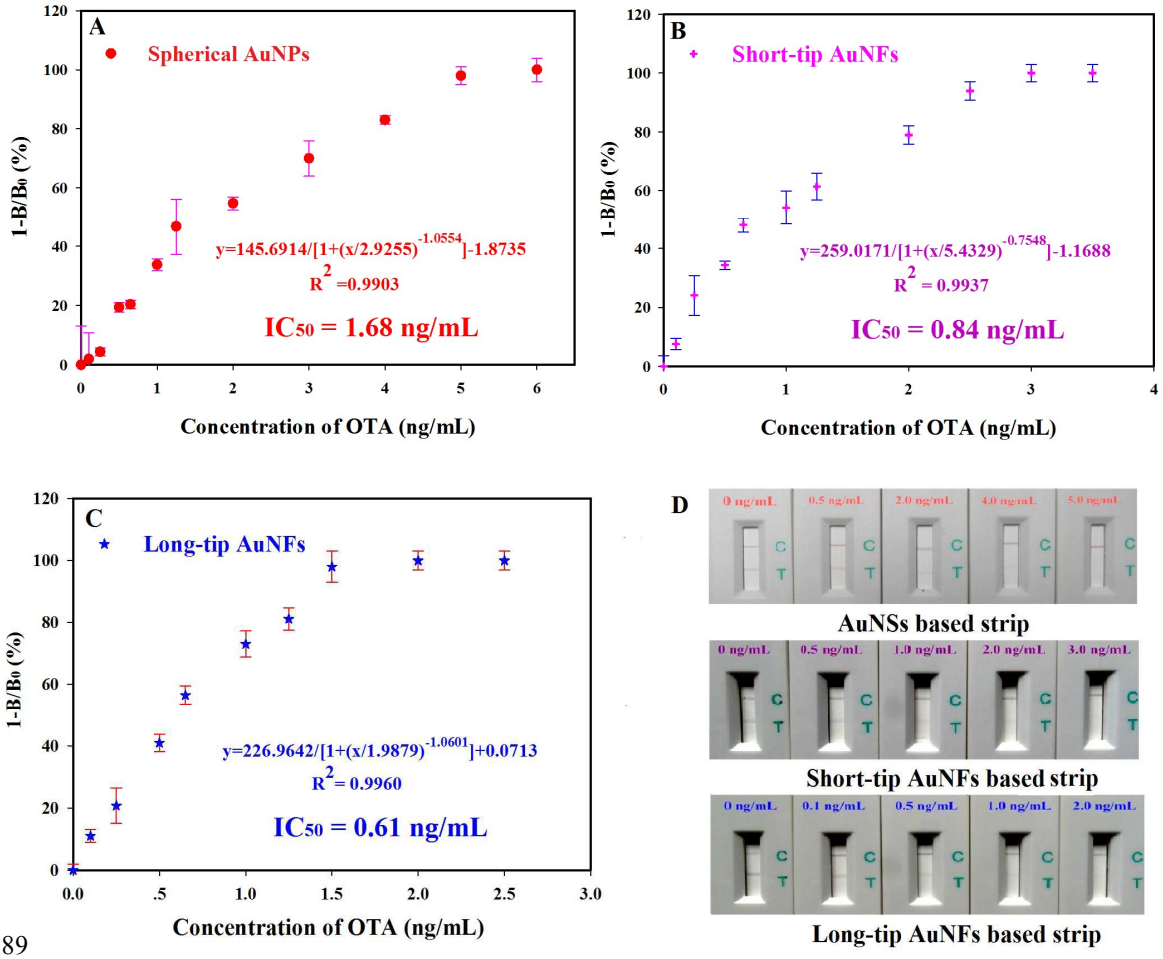

Figure 4. Xu *et al*.

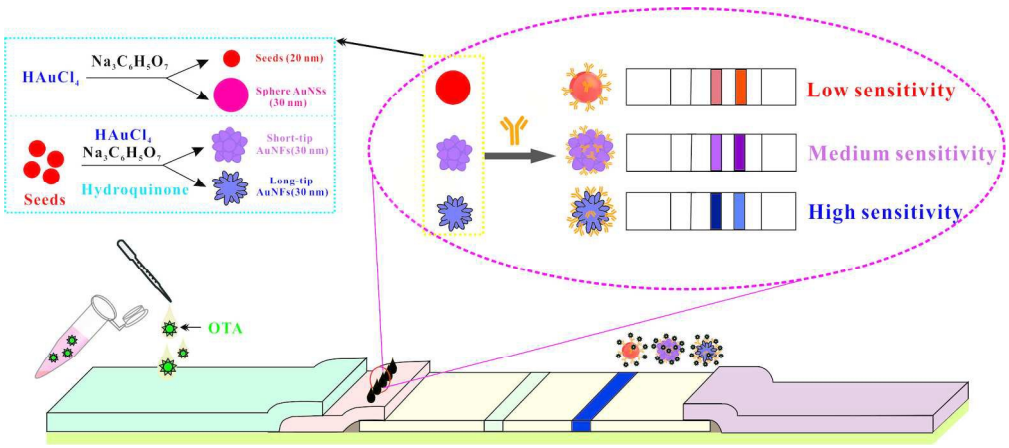

199x87mm (300 x 300 DPI)